

Synthesis of Unsaturated Os₃W₂ and Metastable Os₄W Oxo-Ethylidyne Clusters by Solid-State Pyrolysis. Direct C–O Bond Cleavage of a Coordinated Ketenyl Ligand

Jia-Huey Gong, Der-Kweng Hwang, Chyuan-Wu Tsay, and Yun Chi*

Department of Chemistry, National Tsing Hua University,
Hsinchu 30043, Taiwan, Republic of China

Shie-Ming Peng* and Gene-Hsiang Lee

Department of Chemistry, National Taiwan University,
Taipei 10764, Taiwan, Republic of China

Received December 20, 1993*

Heterometallic ketenyl complex Os₃(CO)₁₀(μ-H)[C(O)CH₂(W(CO)₃Cp)] (**1a**) possessing a pendant CpW(CO)₃ substituent was prepared by condensation of Os₃(CO)₁₀(NCMe)₂ with the metal–aldehyde complex CpW(CO)₃CH₂CHO. Pyrolysis of **1a** in the solid state at 185 °C afforded two heteropentametallic cluster compounds, Cp₂W₂Os₃(CO)₁₂(μ-O)(μ₃-CMe) (**2**) and CpWOs₄(CO)₁₂(μ-O)(μ₃-CMe) (**3**), demonstrating a unique example of C–O bond scission of a ligated ketene fragment and a cluster aggregation process. Complex **2** crystallizes in orthorhombic space group *Pnma* with *a* = 18.913(4) Å, *b* = 16.229(3) Å, *c* = 9.129(2) Å, *Z* = 4, *R* = 0.054, and *R*_w = 0.055 for 2551 observed reflections. The W₂Os₃ cluster that contains 72 cluster valence electrons has a distorted square-pyramidal array of metal atoms with one Os–H–Os hydride ligand, one bridging oxo ligand associated with a W–W double bond, and an ethylidyne ligand bridging a unique W₂Os triangle. Crystals of **3** are monoclinic of space group *P2₁/n* with *a* = 15.941(2) Å, *b* = 19.395(4) Å, *c* = 16.369(4) Å, β = 94.72(2)°, *Z* = 8, *R* = 0.050, and *R*_w = 0.041 for 6568 observed reflections. This molecule possesses a WOs₄ trigonal-bipyramidal skeleton with an oxo ligand bridging a W–Os edge and an ethylidyne ligand capping a WOs₂ face. Isomerization of **3** occurred upon dissolution at room temperature to afford edge-bridging tetrahedral cluster CpWOs₄(CO)₁₂(μ₃-O)(μ₃-CMe) (**4**), in which the oxo ligand formally migrated from an edge-bridging to a face-bridging position. Pyrolysis of **4** in the solid state at 190 °C regenerated **3** in high yield, suggesting the existence of a delicate equilibrium between these two cluster complexes. Crystal data for **4**: space group *P2₁/n*, *a* = 9.492(3) Å, *b* = 16.990(2) Å, *c* = 15.887(3) Å, β = 98.79(2)°, *Z* = 4. The structure was solved by direct methods and refined to *R* and *R*_w values of 0.039 and 0.032 for 4455 observed reflections with *I* > 2σ(*I*).

Solid-state pyrolysis is a process of fundamental significance for the preparation of high nuclearity binary carbonyl clusters.¹ Many polynuclear complexes of the third-row elements have been prepared accordingly, because these carbonyl clusters have a much larger M–M bond energy in relation to the M–CO bond energy; thus they show a greater tendency to aggregate.² For clusters containing a bound hydrocarbon fragment in addition to CO ligands, building a new, condensed cluster framework by this route may also lead to simultaneous rearrangement of hydrocarbyl ligands related to transformations on the surface of a metal catalyst.³ With this idea in mind, we designed the synthesis of a WOs₃ cluster with a pendant ketenyl group (O=C=CH₂) and investigated the chemical transformation of this ketenyl functional group under the conditions of solid-state thermolysis, anticipating finding some novel reactivity patterns for this functional group,

namely cleavage of the C–O bond. The ketenyl group was selected for these experiments, not only because both organic ketenes and organometallic ketenyl complexes have been extensively investigated⁴ but also because ligated ketenes serve as intermediates in the growth of hydrocarbon chains during CO reduction reactions.⁵ Thus the properties of the ligated ketenyl group can be more realistically compared with those of uncomplexed counterparts and provide a critical assessment of cluster/surface analogies.⁶

In this paper, we describe the preparation of a ketenyl complex, Os₃(CO)₁₀(μ-H)[C(O)CH₂W(CO)₃Cp] (**1a**), via a rational reaction of the metal–aldehyde complex CpW(CO)₃CH₂CHO with the triosmium cluster Os₃(CO)₁₀(NCMe)₂. The unsaturated, square-pyramidal CpWOs₄(CO)₁₂(μ-O)(μ₃-CCH₃) (**2**) and metastable trigonal-bipyramidal Cp₂W₂Os₃(CO)₉(μ-O)(μ₃-CCH₃) (**3**) were subsequently prepared by thermolysis of **1a** in the solid state and were characterized by spectroscopic and structural methods. These clusters contain a pair of bridging oxo and ethylidyne ligands; thus their formation provides an

* Abstract published in *Advance ACS Abstracts*, March 15, 1994.

(1) (a) Jackson, P. F.; Johnson, B. F. G.; Lewis, J.; Nelson, W. J. H.; McPartlin, M. *J. Chem. Soc., Dalton Trans.* 1982, 2099. (b) Amoroso, A. J.; Johnson, B. F. G.; Lewis, J.; Raithby, P. R.; Wong, W. T. *J. Chem. Soc., Chem. Commun.* 1990, 1208. (c) Amoroso, A. J.; Gade, L. H.; Johnson, B. F. G.; Lewis, J.; Raithby, P. R.; Wong, W. T. *Angew. Chem., Int. Ed. Engl.* 1991, 30, 107.

(2) Connor, J. A. In *Transition Metal Clusters*; Johnson, B. F. G., Ed.; Wiley: New York, 1981; p 345.

(3) Clauss, A. D.; Shapley, J. R.; Wilker, C. N.; Hoffmann, R. *Organometallics* 1984, 3, 619.

(4) Geoffroy, G. L.; Bassner, S. L. *Adv. Organomet. Chem.* 1988, 28, 1.

(5) Brady, R. C.; Pettit, R. *J. Am. Chem. Soc.* 1980, 102, 6181. (b) Brady, R. C.; Pettit, R. *J. Am. Chem. Soc.* 1981, 103, 1287.

(6) Muetterties, E. L. *Bull. Soc. Chim. Belg.* 1975, 84, 959.

unambiguous example of the cleavage of the C–O double bond, despite the possibility that the ketenyl CO may exchange with coordinated CO ligands of the cluster and this C–O multiple bonding is considered fairly inert under regular conditions. Furthermore, isomerization of metastable **3** proceeded spontaneously in solution at room temperature to afford CpW(Os₄(CO)₁₂(μ₃-O)(μ₃-CCH₃)) (**4**). The latter reverted to **3** on thermolysis at a higher temperature (190 °C) in nearly quantitative yield, providing a rare example of temperature-dependent, reversible cluster core rearrangement. To our knowledge, this is the first example of the generation of metastable cluster complexes under thermal conditions. Related isomerization, which involves photoinduced reorganization of the metal–metal bond of the butterfly framework, has been observed in the heterometallic cluster PtOs₃(CO)₁₀(dppm)-[Si(OMe)₃](μ-H) by Adams and co-workers.⁷

Experimental Procedure

General Information and Materials. Infrared spectra were recorded on a Perkin-Elmer 2000 FT-IR spectrometer. ¹H and ¹³C NMR spectra were recorded on Bruker AM-400 and Varian Gemini-300 instruments; chemical shifts are quoted with respect to internal standard tetramethylsilane (¹H and ¹³C NMR). Mass spectra were obtained on a JEOL-HX110 instrument operating in the fast atom bombardment (FAB) mode. All reactions were performed under a nitrogen atmosphere using deoxygenated solvents dried with an appropriate reagent. The progress of reactions was monitored by analytical thin-layer chromatography (5735 Kieselgel 60 F₂₅₄, Merck), and the products were separated on commercially available preparative thin-layer chromatographic plates (Kieselgel 60 F₂₅₄, Merck). These aldehyde complexes CpW(CO)₃CH₂CHO were prepared from reactions of the CpW(CO)₃⁻ anion and freshly distilled chloroacetaldehyde at 0 °C. Elemental analyses were performed at the NSC Regional Instrumentation Center at National Cheng Kung University, Tainan, Taiwan.

Reaction of Os₃(CO)₁₀(NCMe)₂ with CpW(CO)₃CH₂CHO. A toluene solution (35 mL) of Os₃(CO)₁₀(NCMe)₂ (180 mg, 0.193 mmol) and CpW(CO)₃CH₂CHO (110 mg, 0.293 mmol) was heated at reflux under nitrogen for 30 min, during which time the solution turned from light yellow to orange. After evaporation of the solvent in vacuo, the residue was separated by thin-layer chromatography (TLC) (silica gel, dichloromethane:hexane = 1:2), giving 64 mg of yellow Os₃(CO)₁₀(μ-H)[C(O)CH₂(W(CO)₃Cp)] (**1a**, 0.052 mmol, 27%). A selectively ¹³C enriched sample of **1a**, Os₃(C*O)₁₀(μ-H)[C(O)CH₂(W(C*O)₃Cp)], was prepared from 50% enriched Os₃(C*O)₁₀(NCMe)₂ and CpW(CO)₃CH₂CHO under similar conditions.

Spectral data for **1a**: MS (FAB, ¹⁹²Os, ¹⁸⁴W) *m/z* 1232 (M⁺); IR (C₆H₁₂) ν(CO) 2106 (w), 2066 (vs), 2054 (s), 2030 (m, sh), 2022 (s), 2008 (m), 1999 (vw), 1991 (vw), 1977 (w), 1948 (m), 1937 (s, br) cm⁻¹; ¹H NMR (CDCl₃, 294 K) δ 5.43 (s, 5H), 3.02 (d, 1H, *J*_{H-H} = 6.0 Hz), 2.75 (d, 1H, *J*_{H-H} = 6.0 Hz), -14.07 (s, 1H); ¹³C NMR (CDCl₃, 294 K) (CO) δ 270.7 (CH₂CO), 226.0 (*J*_{W-C} = 125 Hz), 218.3 (*J*_{W-C} = 152 Hz), 217.3 (*J*_{W-C} = 156 Hz), 184.5, 182.2, 178.4, 176.3, 176.1, 176.0, 175.9, 175.0, 174.9, 174.6; ¹³C NMR (CDCl₃, 294 K) δ 91.8 (C₅H₅, 5C), 17.3 (CH₂, *J*_{W-C} = 31 Hz). Anal. Calcd for C₂₀H₈O₁₄Os₃W₁: C, 19.58; H, 0.66. Found: C, 19.40; H, 0.63.

Solid-State Pyrolysis of 1a. Complex **1a** (133 mg, 0.108 mmol) was placed in a 5-mm NMR tube under N₂, and the tube was inserted into a preheated oil bath at 190 °C for 10 min. Under these conditions, complex **1a** melted and turned black. The residue was extracted with dichloromethane and the insoluble material removed by filtration. The filtrate was then concentrated and separated by TLC (silica gel, dichloromethane:hexane

= 1:2), giving 17 mg of orange red CpW(Os₄(CO)₁₂(μ₃-O)(μ₃-CCH₃)) (**3**, 0.012 mmol, 11%) and 15 mg of dark brown Cp₂W₂Os₃(CO)₉(μ₃-O)(μ₃-CCH₃) (**2**, 0.011 mmol, 10%). Crystals of **2** suitable for X-ray diffraction study were obtained from a layered solution of dichloromethane–methanol at room temperature, whereas complex **3** was recrystallized from a mixture of dichloromethane–hexane.

Spectral data for **2**: MS (FAB, ¹⁹²Os, ¹⁸⁴W) *m/z* 1370 (M⁺); IR (C₆H₁₂) ν(CO) 2064 (s), 2032 (vs), 2015 (vs), 2002 (vw), 1989 (m), 1974 (m), 1963 (w), 1960 (m) cm⁻¹; ¹H NMR (CDCl₃, 294 K) δ 6.15 (s, 10H), 3.72 (s, 3H), -19.40 (s, 1H); ¹³C NMR (THF-*d*₈, 294 K) (CO) δ 200.6 (2C, br), 186.6 (2C), 183.3 (2C, br), 182.6, 180.0 (2C, br); ¹³C NMR (THF-*d*₈, 294 K) δ 275.4 (CCH₃, *J*_{W-C} = 104 Hz), 103.4 (C₅H₅, 5C), 53.6 (CH₃). Anal. Calcd for C₂₁H₁₄O₁₀Os₃W₂: C, 18.40; H, 1.03. Found: C, 17.37; H, 0.97.

Spectral data for **3**: MS (FAB, ¹⁹²Os, ¹⁸⁴W) *m/z* 1396 (M⁺); IR (C₆H₁₂) ν(CO) 2094 (w), 2062 (vs), 2037 (m), 2031 (s), 2008 (w), 1996 (vw), 1990 (vw), 1977 (w), 1960 (vw), 1953 (vw) cm⁻¹; ¹H NMR (CD₂Cl₂, 294 K) δ 5.78 (s, 5H), 3.95 (s, 3H); ¹³C NMR (CDCl₃, 294 K) (CO) δ 183.3 (3C), 182.0 (br), 180.8 (3C, br), 179.4 (br), 176.8 (br), 173.1, 172.8, 169.6; ¹³C NMR (CDCl₃, 294 K) δ 222.2 (CCH₃), 100.8 (Cp), 45.2 (CH₃). Anal. Calcd for C₁₉H₈O₁₃Os₄W₁: C, 16.33; H, 0.58. Found: C, 16.48; H, 0.60.

Pyrolysis of 1a in the Presence of CpW(CO)₃H. In a 50-mL pear-shaped reaction flask, complex **1a** (85 mg, 0.069 mmol) and CpW(CO)₃H (42 mg, 0.126 mmol) were first dissolved in 10 mL of dichloromethane to provide a light yellow, homogeneous solution. Then the solvent was removed under vacuum to provide a thin coating on the wall of the reaction flask and allowed to continuously evacuate for another 15 min to ensure complete removal of solvent. Subsequently, the flask was filled with N₂ gas and immersed into a preheated oil bath at 190 °C for 10 min. The residue was extracted with dichloromethane and the mixture was separated by TLC (silica gel, dichloromethane:hexane = 1:2), giving 23 mg of dark brown **2** (0.017 mmol, 25%) in addition to **3** in a trace amount (3 mg, 0.0021 mmol, 3%).

Isomerization of 3. A toluene solution (25 mL) of **3** (20 mg, 0.014 mmol) was stirred at room temperature for 5 days. Then the solvent was evaporated and the residue was separated by TLC (dichloromethane:hexane = 1:2), giving 2.4 mg of **3** (0.0017 mmol, 12%) and 16 mg of **4** (0.011 mmol, 80%).

Spectral data for **4**: MS (FAB, ¹⁹²Os, ¹⁸⁴W) *m/z* 1396 (M⁺); IR (C₆H₁₂) ν(CO) 2088 (w), 2059 (vs), 2036 (vs), 2019 (m), 1995 (w), 1988 (w), 1974 (vw), 1961 (vw), 1942 (vw), 1908 (vw) cm⁻¹; ¹H NMR (CD₂Cl₂, 294 K) δ 6.02 (s, 5H), 3.79 (s, 3H); ¹³C NMR (CDCl₃, 294 K) (CO) δ 194.4, 184.8 (br), 184.2, 182.4, 179.3 (sh), 177.3 (3C), 175.7 (br), 175.1 (sh), 168.4 (br), 168.0 (sh); ¹³C NMR (CDCl₃, 294 K) δ 220.2 (CCH₃), 98.6 (Cp), 44.8 (CH₃). Anal. Calcd for C₁₉H₈O₁₃Os₄W₁: C, 16.33; H, 0.58. Found: C, 16.43; H, 0.59.

Solid-State Pyrolysis of 4. Complex **4** (8 mg, 0.0057 mmol) was placed in a 5-mm NMR tube and heated at 190 °C for 5 min. Then the residue was dissolved in dichloromethane and separated by TLC (silica gel, dichloromethane:hexane = 1:2) to produce 7.5 mg of orange red **3** (0.0054 mmol, 94%).

X-ray Crystallography. Diffraction measurements of complexes **2–4** were carried out on a Nonius CAD-4 diffractometer. All reflections were corrected for Lorentz, polarization, and absorption effects. Data deduction and refinement were performed using the NRCC-SDP-VAX packages.

Lattice parameters of **2** were determined from 25 randomly selected high angle reflections with 2θ angles in the range 18.00–30.36°. Absorption corrections were made by the ψ scan method; the minimum and maximum transmission factors were 0.21 and 1.00, respectively. The crystal decomposed gradually due to loss of CH₂Cl₂ solvent molecule and the intensity of standard reflections decayed 15% during data collection. Anisotropic thermal parameters were introduced for all non-hydrogen atoms. Full matrix least-squares refinement with 28 atoms and 188 parameters gave *R* = 0.054 and *R*_w = 0.055, for 1877 reflections

(7) Adams, R. D.; Cortopassi, J. E.; Aust, J.; Myrick, M. *J. Am. Chem. Soc.* 1993, 115, 8877.

Table 1. Experimental Data for the X-ray Diffraction Studies of 2–4

	2	3	4
compd	2	3	4
formula	C ₂₂ H ₁₅ Cl ₂ O ₁₀ Os ₃ W ₂	C ₁₉ H ₈ O ₁₃ Os ₄ W	C ₁₉ H ₈ O ₁₃ Os ₄ W
mol wt	1448.74	1388.95	1388.95
cryst syst	orthorhombic	monoclinic	monoclinic
space group	<i>Pnma</i>	<i>P2₁/n</i>	<i>P2₁/n</i>
<i>a</i> (Å)	18.913(4)	15.941(2)	9.492(3)
<i>b</i> (Å)	16.229(3)	19.395(4)	16.990(2)
<i>c</i> (Å)	9.129(2)	16.369(4)	15.887(3)
β (deg)		94.72(2)	98.79(2)
<i>V</i> (Å ³)	2802(1)	5044(2)	2532(1)
<i>Z</i>	4	8	4
<i>D_c</i> (g/cm ³)	3.434	3.658	3.644
<i>F</i> (000)	2548	4832	2416
cryst size, mm	0.06 × 0.13 × 0.65	0.05 × 0.10 × 0.40	0.05 × 0.08 × 0.32
<i>h, k, l</i> ranges	0, 22; 0, 19; 0, 10	-17, 17; 0, 20; 0, 17	-11, 11; 0, 20, 0, 18
trans factors: max, min	1.00, 0.21	1.00, 0.57	1.00, 0.36
std reflns	decay 15%	variation ≤3%	variation ≤4%
μ (mm ⁻¹)	21.98	24.82	24.71
no. of unique data ($2\theta_{\max}$ (deg))	2551 (50)	6569 (45)	4455 (50)
no. of params	188	348	335
max Δ/σ ratio	0.041	0.010	0.035
<i>R</i> ; <i>R_w</i>	0.054; 0.055	0.050; 0.041	0.039; 0.032
GOF	2.26	1.70	2.05
residual electron density, e/Å ³	3.43/-2.97	2.01/-2.78	2.36/-2.32

with $I > 2\sigma(I)$. The residual electron density on the difference Fourier map is around 3.43 e/Å³.

Lattice parameters of **3** were determined and refined by a least-squares fit of 25 randomly selected high angle reflections with 2θ angles in the range 16.80–22.88°. The space group *P2₁/n* was identified on the basis of systematic absences and confirmed by solving the crystal structure. The minimum and maximum transmission factors were 0.57 and 1.00, respectively. Anisotropic thermal parameters were introduced for W and Os atoms. Isotropic temperature factors were assigned to all other non-hydrogen atoms. The hydrogen atoms were calculated at idealized positions and were included in the structure factor calculation. Refinement was by full matrix least squares with 90 atoms and 348 parameters, giving *R* = 0.050 and *R_w* = 0.041 for 3404 reflections with $I > 2\sigma(I)$. Weights based on counting statistics were used.

Lattice parameters of **4** were determined from 25 randomly selected high angle reflections with 2θ angles in the range 18.50–26.10°. The space group *P2₁/n* was identified on the basis of systematic absences. Absorption corrections were performed, and the minimum and maximum transmission factors were 0.36 and 1.00, respectively. The structures were solved by direct methods and refined by least-squares cycles, all non-hydrogen atoms were refined with anisotropic thermal parameters. The hydrogen atoms were calculated in idealized positions with a fixed temperature coefficient and included in the structure factor calculation. The combined data collection and refinement parameters are given in Table 1. Atomic positional parameters for 2–4 are presented in Tables 2–4, whereas selected bond angles and lengths are given in Tables 5–7, respectively.

Results and Discussion

Tetranuclear ketenyl compounds Os₃(CO)₁₀(μ -H)-[C(O)CH₂(W(CO)₃Cp)] (**1a**) possessing a pendant CpW(CO)₃ substituent are readily available by condensation of Os₃(CO)₁₀(NCMe)₂ with the aldehyde complex CpW(CO)₃CH₂CHO in refluxing toluene (30 min). Compound **1a** was fully characterized by spectroscopic methods. The key feature is, however, provided by ¹H NMR data which show a hydride signal at δ -14.07 and two methylene signals at δ 3.02 and 2.75 with coupling constant ²*J*_{H-H} = 6.0 Hz. This observation indicates that the aldehyde reagent reacted with the osmium cluster in a manner similar to its organic counterparts, RCHO, R = Me, Ph, etc.⁸ An X-ray diffraction study on this molecule⁹ confirmed that its

Table 2. Atomic Coordinates and Equivalent Isotropic Displacement Coefficients for 2

	<i>x</i>	<i>y</i>	<i>z</i>	<i>B_{eq}</i> ^a (Å ²)
Os(1)	0.74425(8)	1/4	0.15422(15)	2.26(5)
Os(2)	0.70139(5)	0.34319(5)	0.40011(10)	2.40(4)
W	0.60685(5)	0.32861(5)	0.17824(10)	2.37(4)
C(1)	0.7747(15)	0.3381(12)	0.0372(25)	3.7(13)
C(2)	0.7400(14)	0.4366(11)	0.3066(23)	2.8(11)
C(3)	0.6363(17)	0.4024(14)	0.517(3)	4.3(13)
C(4)	0.7762(15)	0.3405(12)	0.550(4)	5.3(16)
C(5)	0.8317(20)	1/4	0.276(5)	5.1(23)
C(6)	0.356(3)	3/4	0.157(5)	6.9(29)
C(7)	0.6465(17)	1/4	0.024(4)	2.5(14)
C(8)	0.5246(17)	0.4389(16)	0.203(3)	6.0(16)
C(9)	0.5958(18)	0.4754(15)	0.198(4)	6.4(18)
C(10)	0.6206(16)	0.4630(15)	0.064(4)	6.5(19)
C(11)	0.5724(22)	0.4137(14)	-0.023(3)	6.5(19)
C(12)	0.5152(17)	0.3988(14)	0.069(3)	5.2(15)
C(13)	0.027(5)	3/4	0.056(6)	13.1(59)
O(1)	0.7968(12)	0.3901(10)	-0.0390(22)	6.0(11)
O(2)	0.7658(12)	0.4914(9)	0.2565(24)	5.6(11)
O(3)	0.5976(12)	0.4409(11)	0.5816(21)	5.7(10)
O(4)	0.8185(12)	0.3428(10)	0.6339(20)	5.6(10)
O(5)	0.8816(14)	1/4	0.335(3)	5.9(16)
O(6)	0.5421(13)	1/4	0.249(3)	3.7(12)
Cl	0.0354(15)	0.6732(13)	0.136(4)	33.7(30)

^a *B_{eq}* is the mean of the principal axes of the thermal ellipsoid.

structure (Chart 1) is analogous to the structurally characterized, parent acetyl complex Os₃(CO)₁₀(μ -H)-[C(O)CH₃], prepared by reaction of Os₃(CO)₁₀(NCMe)₂ and acetaldehyde.¹⁰ In fact, the IR ν (CO) spectrum of **1a** shows a pattern of the CO stretching bands in the region of Os bound CO ligands (2106–1977 cm⁻¹) almost superimposable with that of Os₃(CO)₁₀(μ -H)[C(O)CH₃].

Next, we examined the thermal pyrolysis of **1a** in an attempt to account for the reactivity of the ketenyl group. In these experiments, a solid sample of **1a** was heated under nitrogen at 185–195 °C for 10 min, giving a dark brown pentanuclear oxo-ethylidyne compound Cp₂W₂-Os₃(CO)₉(μ -H)(μ -O)(μ -3-CCH₃) (**2**) in 10% yield and a red oxo-ethylidyne CpWOs₄(CO)₁₂(μ -O)(μ -3-CCH₃) (**3**) in 11%

(8) Azam, K. A.; Deeming, A. J.; Rothwell, I. P. *J. Chem. Soc., Dalton Trans.* 1981, 91.

(9) Selective crystal data for **1a**: monoclinic, space group *I2/a*, *a* = 24.235(4) Å, *b* = 7.820(1) Å, *c* = 29.308(9) Å, β = 91.16(2)°, *Z* = 8, *R* = 0.042 for 3546 reflections with $I \geq 2\sigma(I)$.

(10) Johnson, B. F. G.; Lewis, J.; Odiaka, T. I.; Raithby, P. R. *J. Organomet. Chem.* 1981, 216, C56.

Table 3. Atomic Coordinates and Equivalent Isotropic Displacement Coefficients for 3

	x	y	z	B _{eq} ^a (Å ²)		x	y	z	B _{eq} ^a (Å ²)
W(1A)	0.29674(10)	0.31559(10)	0.34312(12)	2.35(8)	W(1B)	0.78598(10)	0.57309(10)	0.33940(12)	2.10(8)
Os(1A)	0.31055(10)	0.21041(10)	0.24089(11)	2.13(8)	Os(1B)	0.81408(10)	0.46779(9)	0.24108(11)	2.16(8)
Os(2A)	0.24156(10)	0.33309(10)	0.16281(12)	2.53(8)	Os(2B)	0.73081(10)	0.58228(10)	0.15835(11)	2.22(8)
Os(3A)	0.14464(10)	0.26225(10)	0.26227(12)	2.21(8)	Os(3B)	0.64215(10)	0.58228(10)	0.15835(11)	2.22(8)
Os(4A)	0.22773(10)	0.18197(10)	0.38827(11)	2.39(8)	Os(3B)	0.64215(10)	0.50574(9)	0.25908(11)	1.98(8)
C(1A)	0.2738(25)	0.1324(24)	0.172(3)	3.1(10)	Os(4B)	0.73417(10)	0.43563(10)	0.38867(11)	2.27(8)
C(2A)	0.3933(25)	0.1582(24)	0.303(3)	3.2(10)	C(1B)	0.787(3)	0.3826(24)	0.180(3)	3.2(10)
C(3A)	0.385(3)	0.236(3)	0.168(3)	3.7(11)	C(2B)	0.906(3)	0.4293(24)	0.313(3)	3.3(10)
C(4A)	0.337(3)	0.3781(25)	0.129(3)	3.4(10)	C(3B)	0.888(3)	0.4903(25)	0.163(3)	3.3(10)
C(5A)	0.185(4)	0.409(4)	0.120(4)	7.9(18)	C(4B)	0.821(3)	0.6349(24)	0.124(3)	3.2(10)
C(6A)	0.228(3)	0.277(3)	0.070(4)	5.7(14)	C(5B)	0.6645(24)	0.6520(23)	0.109(3)	3.0(10)
C(7A)	0.058(4)	0.310(3)	0.189(4)	7.0(16)	C(6B)	0.7247(24)	0.5242(23)	0.067(3)	2.6(9)
C(8A)	0.1004(24)	0.1779(23)	0.221(3)	2.7(9)	C(7B)	0.5544(24)	0.5439(23)	0.179(3)	2.9(9)
C(9A)	0.080(3)	0.2717(24)	0.349(3)	3.1(10)	C(8B)	0.6096(23)	0.4150(23)	0.222(3)	2.6(9)
C(10A)	0.2087(24)	0.0949(23)	0.344(3)	2.8(9)	C(9B)	0.5755(24)	0.5132(23)	0.350(3)	2.8(9)
C(11A)	0.1534(25)	0.1666(24)	0.469(3)	3.2(10)	C(10B)	0.731(3)	0.3501(25)	0.345(3)	3.4(10)
C(12A)	0.313(3)	0.1434(25)	0.465(3)	3.5(10)	C(11B)	0.6521(22)	0.4119(22)	0.461(3)	2.2(8)
C(13A)	0.159(3)	0.436(3)	0.299(3)	4.4(12)	C(12B)	0.828(3)	0.401(3)	0.469(3)	4.4(12)
C(14A)	0.2062(25)	0.3677(24)	0.275(3)	3.0(10)	C(13B)	0.6330(25)	0.6751(24)	0.284(3)	3.2(10)
C(15A)	0.380(3)	0.418(3)	0.328(3)	3.7(11)	C(14B)	0.6900(20)	0.6149(19)	0.2755(22)	1.0(7)
C(16A)	0.359(3)	0.416(3)	0.414(3)	5.6(14)	C(15B)	0.854(3)	0.682(3)	0.325(3)	4.2(11)
C(17A)	0.405(3)	0.354(3)	0.448(3)	4.9(12)	C(16B)	0.832(3)	0.677(3)	0.399(3)	4.3(11)
C(18A)	0.448(3)	0.324(3)	0.386(3)	4.4(12)	C(17B)	0.874(3)	0.631(3)	0.443(3)	5.4(13)
C(19A)	0.429(3)	0.3617(25)	0.320(3)	3.6(11)	C(18B)	0.925(3)	0.600(3)	0.404(3)	4.7(12)
O(1A)	0.2494(18)	0.0858(17)	0.1344(20)	4.3(7)	C(19B)	0.918(3)	0.629(3)	0.313(3)	4.4(12)
O(2A)	0.4480(21)	0.1321(20)	0.3399(24)	6.1(9)	O(1B)	0.7695(17)	0.3326(17)	0.1463(20)	4.1(7)
O(3A)	0.4458(19)	0.2449(18)	0.1315(21)	4.9(8)	O(2B)	0.9676(17)	0.4228(16)	0.3539(19)	3.6(7)
O(4A)	0.3958(19)	0.4073(18)	0.1125(21)	4.7(8)	O(3B)	0.9400(18)	0.5068(17)	0.1214(20)	4.2(7)
O(5A)	0.1355(22)	0.4475(21)	0.0877(25)	6.9(10)	O(4B)	0.8775(19)	0.6675(18)	0.1019(21)	4.8(8)
O(6A)	0.2213(19)	0.2389(18)	0.0158(21)	5.0(8)	O(5B)	0.6191(20)	0.6870(18)	0.0742(22)	5.1(8)
O(7A)	0.0044(20)	0.3341(20)	0.1544(22)	5.7(9)	O(6B)	0.7126(18)	0.4882(18)	0.0102(21)	4.6(8)
O(8A)	0.0739(20)	0.1257(19)	0.1929(22)	5.6(9)	O(7B)	0.4952(20)	0.5596(19)	0.1405(23)	5.8(9)
O(9A)	0.0374(17)	0.2849(16)	0.4037(19)	3.8(7)	O(8B)	0.5925(18)	0.3583(17)	0.1974(20)	4.4(8)
O(10A)	0.1967(20)	0.0403(19)	0.3166(22)	5.3(9)	O(9B)	0.5326(19)	0.5255(18)	0.4035(21)	4.9(8)
O(11A)	0.0965(18)	0.1536(17)	0.5099(20)	4.4(8)	O(10B)	0.7273(19)	0.2921(19)	0.3247(21)	5.2(9)
O(12A)	0.3715(19)	0.1243(18)	0.5015(21)	4.9(8)	O(11B)	0.6030(17)	0.3972(16)	0.5028(19)	3.8(7)
O(13A)	0.2548(16)	0.2826(15)	0.4359(18)	3.0(6)	O(12B)	0.8832(21)	0.3960(20)	0.5117(23)	6.2(9)
O(13B)	0.7495(15)	0.5407(14)	0.4337(16)	2.2(6)					

yield. This unexpected reaction contrasts sharply with the behavior of the respective Cp* derivative **1b**, which failed to produce the analogous pentanuclear derivatives under similar conditions but gave rise to four distinctive tetrahedral complexes Cp*W₂Os₃(CO)₉(μ-O)(μ₃-CCH₃) (**5**), Cp*W₂Os₃(CO)₁₁(μ₃-CCH₃) (**6**), Cp*W₂Os₃(CO)₁₁(μ₃-CH) (**7**), and Cp*W₂Os₃(CO)₉(μ-O)(μ-H)(μ-CHCH₃) (**8**), all in very low yields.¹¹

Characterization of 2. The ¹H NMR spectrum exhibits three singlets at δ +6.15, +3.72, and -19.40 in an intensity ratio 10:3:1, indicating that this molecule is composed of two CpW fragments, an ethylidyne group, and a bridging hydride on an Os-Os edge. The ¹³C NMR spectrum at room temperature shows five Os-CO resonances at δ 200.6, 186.6, 183.3, 182.6, and 180.0 with the ratio 2:2:2:1:2, confirming that this molecule has C_s symmetry in solution. The signals of the ethylidyne α- and β-carbon atoms appear at δ 275.4 (*J*_{W-C} = 104 Hz) and 53.6, respectively. The intensity of the tungsten satellites of the α-carbon indicates that the ethylidyne ligand is coordinated to two tungsten atoms in an equivalent chemical environment and the value of the chemical shift is within the range expected for a μ₃-bonding mode.¹² On the basis of these spectroscopic data and FAB mass analysis, we tentatively assigned the formulation Cp₂W₂Os₃(CO)₉(μ-H)(μ-O)(μ₃-CCH₃) to the product.

X-ray diffraction of **2** has been carried out to confirm the identification. Suitable single crystals of **2** were grown from a dichloromethane-methanol solution, but they decomposed rapidly upon removal from the solution, due to loss of CH₂Cl₂ solvent molecule. Greater stability was observed when the crystal was sealed immediately in a capillary tube; in this manner, data collection was accomplished with only a 15% reduction in intensity. As shown in Figure 1, the molecule has a W₂Os₃ square-pyramidal arrangement and possesses a crystallographically imposed plane of symmetry which passes atom Os(1) and bisects the W-W' and the Os(2)-Os(2)' bonds. The ethylidyne grouping was found to lie on this mirror plane and the oxo ligand bridges the W-W' bond. The bond distances associated with the oxo and tungsten atoms (W-W' = 2.552(2) Å and W-O(6) = 1.88(2) Å) indicate the W-W bond to be best considered a double bond;¹³ the respective W-O bonds have a bond order 1.5. The local arrangement of the W(μ-O)W fragment resembles that of the phenylimido ligand in Cp₂W₂Ru₂(CO)₆(μ-NPh)-(CH=CPh)¹⁴ and the doubly bridging alkylidyne ligand in clusters Cp₂W₂Os(CO)₅(μ-C(Tol))(μ₃-C(Tol))¹⁵ and Cp₂W₂Re(CO)₃(μ-Br)(μ-X)(μ-C(Tol))(μ₃-C(Tol)) (X = O and CO).¹⁶ In these cases, an isostructural, symmetrical

(13) Cotton, F. A.; Walton, R. A. *Multiple Bonds between Metal Atoms*; Wiley: New York, 1982; Chapter 6.

(14) Chi, Y.; Liu, L.-K.; Huttner, G.; Zsolnai, L. *J. Organomet. Chem.* **1990**, *390*, C50.

(15) Chi, Y.; Shapley, J. R. *Organometallics* **1985**, *4*, 1900.

(16) Carriedo, G. A.; Jeffery, J. C.; Stone, F. G. A. *J. Chem. Soc., Dalton Trans.* **1984**, 1597.

(11) Gong, J.-H.; Chen, C.-C.; Chi, Y.; Wang, S.-L.; Liao, F.-L. *J. Chem. Soc., Dalton Trans.* **1993**, 1829.

(12) Evans, J.; McNulty, S. C. *J. Chem. Soc., Dalton Trans.* **1984**, 79.

Table 4. Atomic Coordinates and Equivalent Isotropic Displacement Coefficients for 4

	x	y	z	B_{eq}^a (Å ²)
Os(1)	0.11337(8)	0.63585(4)	0.15321(5)	2.38(3)
Os(2)	-0.05898(8)	0.54437(4)	0.24501(5)	2.18(3)
Os(3)	-0.09684(8)	0.71219(4)	0.23702(5)	2.04(3)
Os(4)	-0.05562(8)	0.67623(4)	0.41275(5)	2.12(3)
W	0.16180(8)	0.64387(4)	0.32044(5)	1.89(3)
C(1)	0.2344(24)	0.7182(10)	0.1382(14)	4.2(12)
C(2)	0.2401(23)	0.5578(10)	0.1348(12)	3.8(10)
C(3)	0.010(3)	0.6319(11)	0.0370(14)	4.9(13)
C(4)	0.0377(20)	0.4521(10)	0.2531(11)	2.7(9)
C(5)	-0.1300(22)	0.5179(10)	0.1285(13)	3.5(10)
C(6)	-0.2262(21)	0.5037(10)	0.2820(14)	3.5(10)
C(7)	-0.2562(24)	0.6691(10)	0.1470(17)	5.7(14)
C(8)	-0.0317(22)	0.7944(10)	0.1667(14)	3.9(10)
C(9)	-0.2358(22)	0.7760(11)	0.2735(12)	3.8(10)
C(10)	-0.2177(20)	0.6236(11)	0.4422(13)	3.5(10)
C(11)	-0.1141(21)	0.7746(10)	0.4458(13)	3.4(10)
C(12)	0.0514(20)	0.6573(9)	0.5215(11)	2.7(9)
C(13)	0.0788(17)	0.7457(9)	0.3383(11)	2.2(7)
C(14)	0.1174(22)	0.8324(10)	0.3574(14)	3.7(10)
C(15)	0.3872(21)	0.7012(10)	0.3545(14)	3.8(10)
C(16)	0.4053(18)	0.6367(12)	0.2996(14)	4.0(11)
C(17)	0.3689(22)	0.5681(10)	0.3518(17)	4.8(13)
C(18)	0.3425(18)	0.5949(10)	0.4307(12)	3.0(9)
C(19)	0.3544(21)	0.6758(11)	0.4299(12)	3.5(10)
O(1)	0.3143(18)	0.7677(8)	0.1226(11)	6.5(10)
O(2)	0.3308(17)	0.5112(8)	0.1261(10)	5.7(9)
O(3)	-0.0452(17)	0.6319(10)	-0.0327(9)	6.9(9)
O(4)	0.1155(15)	0.3973(7)	0.2586(11)	5.3(9)
O(5)	-0.1820(17)	0.4974(8)	0.0660(10)	6.1(9)
O(6)	-0.3317(16)	0.4806(9)	0.2987(14)	7.8(12)
O(7)	-0.3431(17)	0.6535(10)	0.1001(12)	8.2(11)
O(8)	0.0056(17)	0.8477(7)	0.1348(9)	5.1(8)
O(9)	-0.3269(17)	0.8137(9)	0.2926(11)	6.9(10)
O(10)	-0.3161(15)	0.5901(9)	0.4618(11)	5.8(9)
O(11)	-0.1452(18)	0.8336(8)	0.4712(10)	5.8(9)
O(12)	0.1199(15)	0.6456(8)	0.5871(9)	5.2(8)
O(13)	0.0394(11)	0.5737(5)	0.3699(7)	1.9(5)

Table 5. Selected Bond Distances (Å) and Bond Angles (deg) for 2 (Esd's in Parentheses)

W-Os(1)	2.903(2)	W-Os(2)	2.712(1)
W-W'	2.552(2)	Os(1)-Os(2)	2.825(2)
Os(2)-Os(2)'	3.025(2)	W-O(6)	1.88(2)
W-C(7)	2.05(3)	Os(1)-C(7)	2.20(3)
C(6)-C(7)	1.65(6)		
W-O(6)-W'	85(1)	W-C(7)-W'	77(1)
W-C(7)-Os(1)	86(1)	Os(1)-C(1)-O(1)	176(2)
Os(1)-C(5)-O(5)	175(4)	Os(2)-C(2)-O(2)	176(2)
Os(2)-C(3)-O(3)	177(2)	Os(2)-C(4)-O(4)	177(2)

Table 6. Selected Bond Distances (Å) and Bond Angles (deg) for 3 (Esd's in Parentheses)

W(1)-Os(1)	2.659(3)	W(1)-Os(2)	3.029(3)
W(1)-Os(3)	2.859(2)	W(1)-Os(4)	2.934(3)
Os(1)-Os(2)	2.876(3)	Os(1)-Os(3)	2.878(2)
Os(1)-Os(4)	2.897(3)	Os(2)-Os(3)	2.709(3)
Os(3)-Os(4)	2.825(3)	W(1)-O(13)	1.82(3)
Os(2)-O(13)	2.13(3)	Os(2)-C(14)	2.07(4)
W(1)-C(14)	2.02(4)	Os(3)-C(14)	2.27(4)
C(13)-C(14)	1.59(7)		
Os(1)-C(1)-O(1)	176(4)	Os(1)-C(2)-O(2)	173(4)
Os(1)-C(3)-O(3)	165(4)	Os(2)-C(4)-O(4)	176(4)
Os(2)-C(5)-O(5)	165(6)	Os(2)-C(6)-O(6)	175(5)
Os(3)-C(7)-O(7)	172(5)	Os(3)-C(8)-O(8)	178(4)
Os(3)-C(9)-O(9)	173(4)	Os(4)-C(10)-O(10)	179(3)
Os(4)-C(11)-O(11)	168(4)	Os(4)-C(12)-O(12)	169(4)

edge-bridging ligand sitting on the W=W double bond was documented (Chart 2).

Furthermore, the bridging hydride ligand was found to be associated with the unique Os(2)-Os(2)' bond because of its elongated bond length (3.029(3) Å) and the dispersed

Table 7. Selected Bond Distances (Å) and Bond Angles (deg) for 4 (Esd's in Parentheses)

Os(1)-Os(2)	2.819(1)	Os(1)-Os(3)	2.872(1)
W-Os(1)	2.630(1)	Os(2)-Os(3)	2.874(1)
W-Os(2)	2.814(1)	Os(3)-Os(4)	2.826(1)
W-Os(3)	2.852(1)	W-Os(4)	2.764(1)
W-O(13)	1.92(1)	Os(2)-O(13)	2.12(1)
Os(4)-O(13)	2.12(1)	W-C(13)	1.94(2)
Os(3)-C(13)	2.21(2)	Os(4)-C(13)	2.21(2)
C(13)-C(14)	1.54(2)		
Os(1)-C(1)-O(1)	174(2)	Os(1)-C(2)-O(2)	175(2)
Os(1)-C(3)-O(3)	176(2)	Os(2)-C(4)-O(4)	172(2)
Os(2)-C(5)-O(5)	172(2)	Os(2)-C(6)-O(6)	175(2)
Os(3)-C(7)-O(7)	173(2)	Os(3)-C(8)-O(8)	171(2)
Os(3)-C(9)-O(9)	176(2)	Os(4)-C(10)-O(10)	179(2)
Os(4)-C(11)-O(11)	176(2)	Os(4)-C(12)-O(12)	178(2)

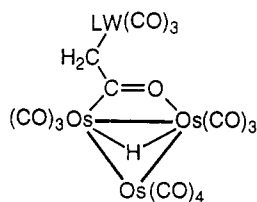
disposition of the CO ligands about this Os-Os edge. Assuming that the neutral oxo ligand is a four-electron donor, we calculate that this molecule possesses 72 cluster valence electrons. This electron counting agrees with the prediction for square-pyramidal clusters with one metal-metal double bond and seven single bonds.^{17,18}

Characterization of 3. This complex shows a molecular ion in its FAB mass spectrum, corresponding to a formula CpW₄Os₄(CO)₁₂(μ-O)(μ₃-CCH₃), and fragmentation ions with successive loss of CO ligands. The solution IR spectrum exhibits 10 CO stretching bands between 2094 and 1953 cm⁻¹, suggesting the presence of terminal CO ligands exclusively. The ¹H NMR spectrum shows two signals at δ 5.78 and 3.95 in a ratio 5:3, confirming the presence of only one CpW fragment and an ethylidyne ligand. The pattern of the CO resonances in the ¹³C NMR spectrum is informative and suggests the presence of four Os(CO)₃ vertices. Two Os(CO)₃ units undergo rapid localized 3-fold rotation and thus exhibit two CO signals at δ 183.3 and 180.8 in the ratio 3:3. The third Os(CO)₃ unit undergoes slow CO exchange, showing three sharp signals at δ 173.1, 172.8, and 169.6 with the ratio 1:1:1. The other Os(CO)₃ unit is evident from the presence of three broad CO signals at δ 182.0, 179.4, and 176.8.

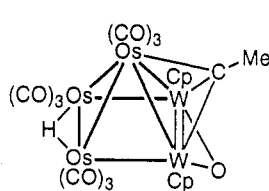
The structure of **3** has been determined by single-crystal X-ray analysis. The molecules crystallized in a monoclinic system with space group *P*2₁/*n*, and the asymmetric unit contains two crystallographically distinct, but structurally similar molecules. An ORTEP diagram is shown in Figure 2, and selected bond parameters for one molecule are presented in Table 6. The metal core consists of a WOs₄ trigonal-bipyramidal arrangement, with atoms Os(2) and Os(4) defining the axial positions and atoms Os(1), Os(3), and W(1) the equatorial positions. The W(1) atom carries a Cp* ligand, and each osmium atom is associated with three terminal CO ligands. The metal-metal distances span a large range 3.029(3)-2.659(3) Å. The two longest metal-metal distances in **3** (3.029(3), 2.934(3) Å) link the tungsten atom to the two apical osmium atoms, while the shortest metal-metal interaction is the W(1)-Os(1) bond (2.659(3) Å) in the equatorial plane. A similar variation in the length of the W-Os vectors, particularly the shortening of the unbridged W-Os bond, was observed for several WOs₃ oxo-alkylidyne clusters.¹⁹ The remaining Os-Os distances range from 2.897(3) to 2.709(3) Å and as

(17) Mingos, D. M. P. *Acc. Chem. Res.* 1984, 17, 311.(18) Wade, K. *Adv. Inorg. Radiochem.* 1976, 18, 1.(19) (a) Chi, Y.; Shapley, J. R.; Churchill, M. R.; Fettingger, J. C. *J. Organomet. Chem.* 1989, 372, 273. (b) Churchill, M. R.; Ziller, J. W.; Beaman, L. R. *J. Organomet. Chem.* 1985, 287, 234.

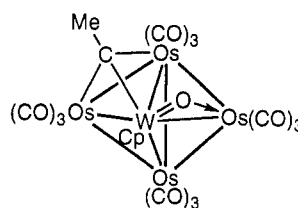
Chart 1



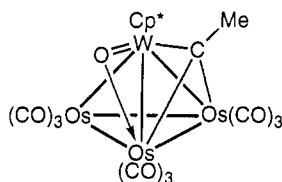
L = Cp, 1a; L = Cp*, 1b



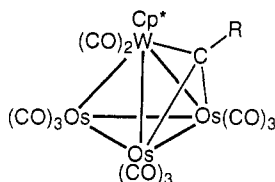
2



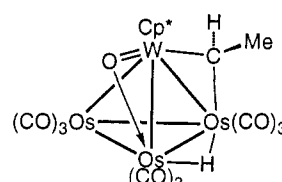
3



5



R = Me, 6; R = H, 7



8

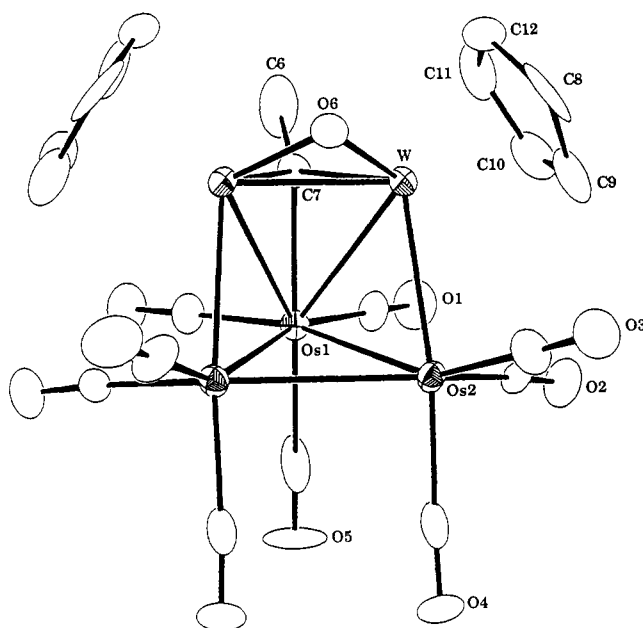
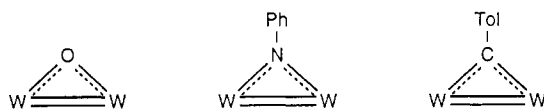


Figure 1. Molecular structure of Cp₂W₂Os₃(CO)₉(μ-H)(μ-O)(μ₃-CCH₃) (2).

Chart 2



such are essentially equivalent to 2.877 Å, the average distance in Os₃(CO)₁₂.²⁰

The ethylidyne ligand bridges the Os(2)—Os(3)—W(1) face, with the Os(3)—C(14) distance (2.27(4) Å) being substantially longer than the other two, W(1)—C(14) = 2.02(4) Å and Os(2)—C(14) = 2.07(4) Å. The oxo ligand is associated with the W(1)—Os(4) edge with a short W—O distance (W(1)—O(13) = 1.82(3) Å) and long Os—O distance (Os(4)—O(13) = 2.13(3) Å). This bonding parameter indicates that the oxo ligand adopts an asymmetrical W=O→Os mode that serves as a four-electron donor.²¹ However, if we accept this concept, the total number of valence electrons of this cluster becomes 74,

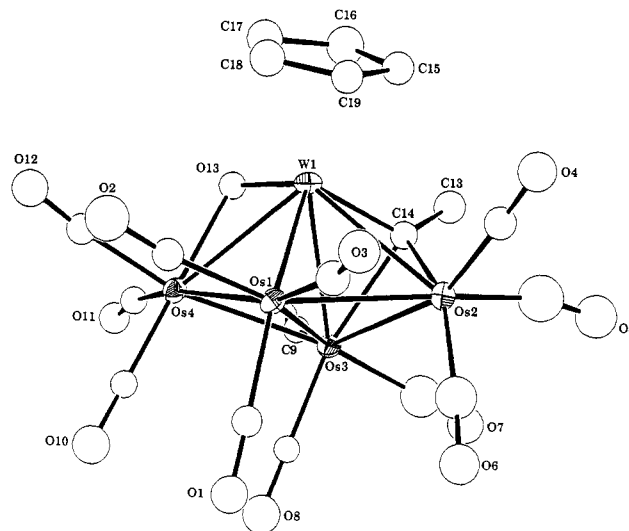


Figure 2. Molecular structure of CpWOs₄(CO)₁₂(μ-O)(μ₃-CCH₃) (3).

which is two electrons in excess of that expected for a cluster with a trigonal-bipyramidal geometry (nine M—M bonds). We do not understand how to account for these two extra electrons in terms of existing theory, but it is possible that the additional pair of electrons resides in a delocalized, weakly metal—metal or metal—ligand antibonding orbital so that the cluster retains its trigonal-bipyramidal geometry. Another possibility is that the oxo ligand may serve as a two-electron instead of a four-electron donor. The latter is supported by the observation reported for the related tetranuclear dioxo complex CpWOs₃(CO)₉(μ-H)(μ-O)₂,²² in which the oxo ligands were invoked to donate six electrons in total to satisfy the electron counting, although they exhibit all the key features of the W=O→Os mode.

Conversion between Complexes 3 and 4. An investigation of the reactivity of electron-rich, metastable complex 3 has been carried out. A sample of 3, dissolved in toluene-*d*₈ solution at room temperature, shows a clean and gradual formation of a new derivative CpWOs₄(CO)₁₂-

(21) (a) Churchill, M.-R.; Bueno, C.; Park, J. T.; Shapley, J. R. *Inorg. Chem.* 1984, 23, 1017. (b) Chi, Y.; Shapley, J. R.; Churchill, M.-R.; Li, Y.-J. *Inorg. Chem.* 1986, 25, 4165.

(22) Chi, Y.; Hwang, L.-S.; Lee, G.-H.; Peng, S.-M. *J. Chem. Soc., Chem. Commun.* 1988, 1456.

(20) Churchill, M. R.; Deboer, B. G. *Inorg. Chem.* 1977, 16, 878.

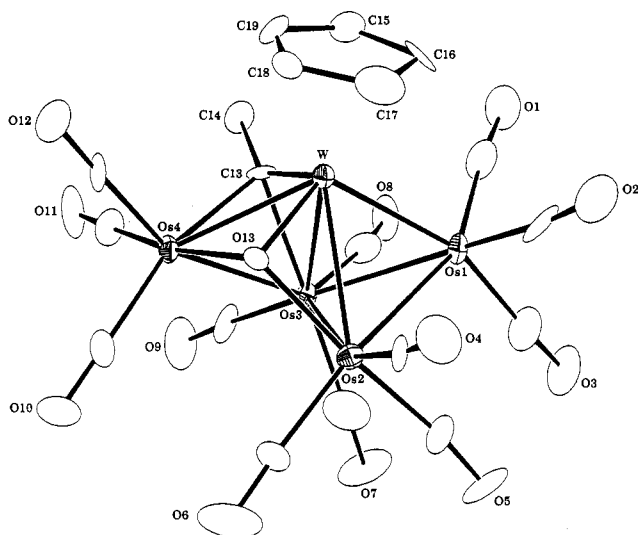


Figure 3. Molecular structure of $\text{CpWOs}_4(\text{CO})_{12}(\mu_3\text{-O})(\mu_3\text{-CCH}_3)$ (**4**).

$(\mu_3\text{-O})(\mu_3\text{-CCH}_3)$ (**4**), which is in equilibrium with complex **3** in a ratio of 35:1, after a period of about 5 days. Complex **4** can be purified by thin-layer chromatography, followed by recrystallization. The FAB mass spectrum exhibits a parent ion identical to that of **3**, confirming that the observed reaction involves no dissociation of a CO ligand. The rate of isomerization was also assessed by ^1H NMR spectroscopy. The analysis, according to reversible first-order kinetics, gives excellent fits of equilibrium and rate constants: $K_{\text{eq}} = [\text{3}]/[\text{4}] = 39(2)$, $k_{\text{obs}} = 3.2(2) \times 10^{-2} \text{ s}^{-1}$. Isomerization performed at higher temperatures produced a similar mixture of complexes **3** and **4**, but the relative ratio altered from 1:35 at room temperature to 1:6 at 60 °C and finally to 3:1 at 90 °C. In agreement with the altered equilibrium ratio, heating of **4** in the solid state at 180 °C for 5 min regenerated **3** in nearly quantitative yield. Furthermore, this temperature-dependent isomerization conforms to the result that no **4** but only **3** was observed during the thermolysis of **1a**.

Characterization of 4. An ORTEP drawing of the molecular structure of **4** appears in Figure 3; selected bond parameters are presented in Table 7. The core of metal atoms consists of a group of three osmium and one tungsten atom arranged in the form of a distorted WOs_3 tetrahedron with an additional $\text{Os}(\text{CO})_3$ group bridging one W-Os edge. The pendant $\text{Os}(\text{CO})_3$ group lies on the extension of the $\text{W-Os}(1)\text{-Os}(3)$ triangle: the dihedral angle between the $\text{W-Os}(1)\text{-Os}(3)$ and $\text{Os}(1)\text{-Os}(3)\text{-Os}(4)$ planes is 15.47(4)°. In this molecule the Os-Os bonds extend from 2.874(1) to 2.819(1) Å, while the W-Os distances span the greater range 2.630(1)–2.852(1) Å. The $\text{W-Os}(1)$ edge, which lies approximately opposite the W-C vector of ethylidyne and the W-O bond of the oxo ligand, is significantly shorter than the other W-Os bonds. The ethylidyne bridges the $\text{W-Os}(3)\text{-Os}(4)$ metal triangle with distances $\text{W-C}(13) = 1.94(2)$, $\text{Os}(3)\text{-C}(13) = 2.21(2)$, and $\text{Os}(4)\text{-C}(13) = 2.21(2)$ Å. The oxo ligand spans the $\text{W-Os}(2)$ edge of the tetrahedron and one Os-Os bond to the $\text{Os}(4)$ atom with distances $\text{W-O}(13) = 1.92(1)$, $\text{Os}(2)\text{-O}(13) = 2.12(1)$, and $\text{Os}(4)\text{-O}(13) = 2.12(1)$ Å; these parameters are characteristic of a face-bridging oxo ligand and indicate the occurrence of a single-bond interaction to all three metal atoms.²³ The related edge-bridging tetrahedral cluster skeleton has been observed in the heterometallic compound $\text{PtOs}_4(\text{CO})_{15}(\mu\text{-H})_2$, which consists of a PtOs_3

tetrahedron and a pendant $\text{Os}(\text{CO})_4$ grouping associated with an Os-Os bond.²⁴ The pentaosmium cluster $\text{Os}_5(\text{CO})_{16}(\mu\text{-H})_2$ also has an edge-bridging tetrahedral skeleton.²⁵

Discussion. In this work the scission of the ketenyl C-O bond and concurrent thermally induced formation of a pair of oxo and ethylidyne ligands have been unambiguously established. Our approach is complementary to several experiments on the ketenyl group in the literature.⁴ These experiments involve isomerization of ketene to formylmethylene²⁶ and dehydration of ketene to afford a ligated acetylide fragment.²⁷ Further examples include treatment of ligated ketene with alcohol that led to formation of acetate,²⁸ whereas reaction with dihydrogen gave an aldehyde,²⁹ reactions with electrophiles, such as H^+ or Me^+ reagent, gave acyl and vinyl ligands,³⁰ and reactions with methylene afforded an oxallyl ligand,³¹ respectively. On the other hand, C-O bond scission in the face-bridging acyl ligand of both WOs_3 and MoOs_3 rhomboidal clusters is documented.³² These clusters gave off two CO molecules upon treatment with Me_3NO followed by heating in refluxing toluene to afford the tetrahedral clusters $\text{CpMOs}_3(\text{CO})_9(\mu\text{-O})(\mu_3\text{-CCH}_2\text{Tol})$, $\text{M} = \text{W}, \text{Mo}$. Other related investigations have shown that ligated cyclopentanone is susceptible to C-O bond cleavage at the tungsten center, leading to formation of oxo and cyclopentylidene fragments.³³ These C-O bond cleavage reactions are presumably favored by the generation of strong multiple bonding between tungsten and oxygen atoms.³⁴

Formation of pentanuclear **2** and **3** is nonstoichiometric and depends greatly on the ancillary ligand and reaction conditions. In our previous investigation, the presence of the bulky and better electron-releasing Cp^* ligand afforded only the tetranuclear derivatives **5**–**8**, whereas when the Cp^* ligand was replaced by a Cp ligand, the expected tetranuclear derivatives disappeared, giving instead pentametallic W_2Os_3 and WOs_4 complexes **2** and **3**, respectively. The products isolated from pyrolysis of both **1a** and **1b** are either clusters containing oxo and alkylidyne ligands or clusters generated indirectly from cleavage of the C-O bond, the latter are complexes **6**–**8** (Chart 1). Among these three products, compound **8** is an ethylidyne cluster, which is formally derived from a secondary addition of a dihydrogen molecule to oxo-alkylidyne cluster **5**, while the alkylidyne clusters **6** and **7** are

(23) (a) Bottomley, F.; Sutin, L. *Adv. Organomet. Chem.* **1988**, *28*, 339. (b) Voss, E. J.; Sabat, M.; Shriver, D. F. *Inorg. Chem.* **1991**, *30*, 2707.

(24) Adams, R. D.; Pompeo, M. P.; Wu, W. *Inorg. Chem.* **1991**, *30*, 2899.

(25) John, G. R.; Johnson, B. F. G.; Lewis, J.; Nelson, W. J.; McPartlin, M. *J. Organomet. Chem.* **1979**, *171*, C14.

(26) Doherty, N. M.; Filders, M. J.; Forrow, N. J.; Knox, S. A. R.; Macpherson, K. A.; Orpen, A. G. *J. Chem. Soc., Chem. Commun.* **1986**, 1335.

(27) Chen, M.-C.; Tsai, Y.-J.; Chen, C.-T.; Lin, Y.-C.; Tseng, T.-W.; Lee, G.-H.; Wang, Y. *Organometallics* **1991**, *10*, 378.

(28) (a) Messerle, L.; Curtis, M. D. *J. Am. Chem. Soc.* **1980**, *102*, 7789. (b) Morrison, E. D.; Geoffroy, G. L. *J. Am. Chem. Soc.* **1985**, *107*, 3541.

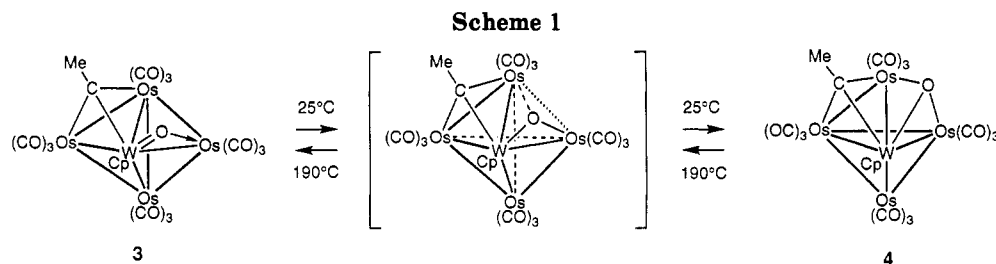
(29) Miyashita, A.; Shitara, H.; Nohira, H. *Organometallics* **1985**, *4*, 1463.

(30) Bassner, S. L.; Morrison, E. D.; Geoffroy, G. L.; Rheingold, A. L. *J. Am. Chem. Soc.* **1986**, *108*, 5358.

(31) Holmgren, J. S.; Shapley, J. R.; Wilson, S. R.; Pennington, W. T. *J. Am. Chem. Soc.* **1986**, *108*, 508.

(32) (a) Shapley, J. R.; Park, J.-T.; Churchill, M. R.; Ziller, J. W.; Beanan, L. R. *J. Am. Chem. Soc.* **1984**, *106*, 1144. (b) Park, J.-T.; Chung, M.-K.; Chun, K. M.; Yun, S. S.; Kim, S. *Organometallics* **1992**, *11*, 3313.

(33) Bryan, J. C.; Mayer, J. M. *J. Am. Chem. Soc.* **1987**, *109*, 7213. (34) Sanderson, R. T. *Inorg. Chem.* **1986**, *25*, 3518.



presumably produced by an intermolecular C–O bond cleavage process, albeit in very low yield.

Exchange between the ketyl CO group and other coordinated CO ligands occurs under the conditions examined. This is evidenced by pyrolysis of a selective ¹³C enriched sample of **1a**, which afforded ¹³C enriched complexes **2** and **3**. Analysis of their ¹³C NMR data suggested that the ethylidyne α -carbon has incorporated a substantial amount of ¹³C isotope and its relative intensity reaches 25–45% of the average intensity of a ¹³C enriched Os–CO ligand. This labeling study has shown that, although the CO exchange is feasible, over half of the ketyl CO ligand has still retained the bonding with the methylene group and converted to give the ethylidyne ligand. This part of the result is relevant to the previously reported reversible conversion between Os₃(CO)₁₁(μ -CH₂) and Os₃(CO)₁₂(μ -CH₂CO).³⁵ Furthermore, the stoichiometry of **3** suggests that its formation may involve condensation of an unidentified WOs₃ intermediate generated directly from **1a**, and a CpW(CO)_xH unit which is produced in a trace amount due to decomposition. This speculation was verified and confirmed because thermolysis of **1a** in the presence of excess CpW(CO)₃H improved the yield from 10% to 23% and suppressed formation of **3** ($\leq 3\%$). Thermolysis of a pulverized mixture of **1a** and Os₃(CO)₁₀(NCMe)₂ in equal proportion resulted in essentially no alteration of isolable yields of **2** and **3**.

Of further interest are the structure and reactivity of clusters **2** and **3**. Complex **2** contains 72 valence electrons (eight M–M bonds); thus it is unsaturated and requires the formation of a metal–metal double bond. In contrast, complex **3** contains 74 valence electrons (nine M–M bonds); thus it is electron-rich with respect to that expected for clusters with trigonal-bipyramidal geometry, as predicted by polyhedral skeletal electron pair theory.¹⁷ Its reactivity pattern confirms the electron-rich and energetically unstable nature of the cluster framework: although cluster **3** is stable indefinitely in the solid state, upon dissolution at room temperature, it slowly converted into an edge-bridging tetrahedral form in nearly quantitative yield, via opening of an Os–Os bond and simultaneous transformation of the ligated oxo atom from an edge-bridging to face-bridging mode. Evidently, the driving force is adoption of an appropriate molecular geometry that can accommodate the additional pair of electrons.

The exact mechanism of the interconversion between **3** and **4** is uncertain, but it may involve a sequence of re-

arrangement from a trigonal-bipyramidal to a square-pyramidal and then to an edge-bridging tetrahedral cluster core. A schematic representation of the detailed processes is shown in Scheme 1, in which the transformation can be viewed as a core rearrangement from trigonal-bipyramidal to square-pyramidal and back to trigonal-bipyramidal; the dashed lines indicate bonds being formed or broken. We proposed that the first step may involve elongation of the unique Os–Os bond in the equatorial plane and gradual formation of a new Os–Os interaction between two Os atoms at the axial positions. Subsequent shifting of the oxo ligand from the edge-bridging mode to a face-bridging mode and cleavage of the Os–Os bond on the same WOs₂ metal triangle complete the transformation. Reversion of this process would regenerate isomer **3**, which is more stable at higher temperatures. Another pathway of isomerization, such as migration of the oxo ligand from the W–Os edge in **3** to the nearby WOs₂ triangular surface followed by cleavage of the Os–Os bond to afford **4**, cannot be excluded on the basis of available data.

Finally, this work also demonstrated a systematic method to prepare high nuclearity transition-metal clusters, through addition of one group 6 metal atom to the existing group 8 trinuclear clusters. The tungsten aldehyde reagent CpW(CO)₃CH₂CHO utilized in this study, together with previously reported alkylidyne complexes CpW(CO)₂(\equiv CR) by Stone and co-workers,³⁶ the hydride complex CpW(CO)₃H,³⁷ and acetylide complexes CpW(CO)₃(C \equiv CR)³⁸ represent useful building blocks in the construction of heterometallic clusters.

Acknowledgment. We thank the National Science Council of the Republic of China for financial support (Grant No. NSC83-0208-M007-43).

Supplementary Material Available: Tables of nonessential bond distances and angles and anisotropic thermal parameters for **2–4** (12 pages). Ordering information is given on any current masthead page.

OM9308654

(36) (a) Delgado, E.; Jeffery, J. C.; Stone, F. G. A. *J. Chem. Soc., Dalton Trans.* **1986**, 2105. (b) Park, J. T.; Shapley, J. R.; Churchill, M. R.; Bueno, C. *Inorg. Chem.* **1983**, *22*, 1579. (c) Stone, F. G. A.; Williams, M. L. *J. Chem. Soc., Dalton Trans.* **1988**, 2467.

(37) (a) Chi, Y.; Wu, F.-J.; Liu, B.-J.; Wang, C.-C.; Wang, S.-L. *J. Chem. Soc., Chem. Commun.* **1989**, 873. (b) Chi, Y.; Chuang, S.-H.; Chen, B.-F.; Peng, S.-M.; Lee, G.-H. *J. Chem. Soc. Dalton Trans.* **1990**, 3033.

(38) (a) Chi, Y.; Lee, G.-H.; Peng, S.-M.; Wu, C.-H. *Organometallics* **1989**, *8*, 1574. (b) Chi, Y.; Hsu, S.-F.; Peng, S.-M.; Lee, G.-H. *J. Chem. Soc., Chem. Commun.* **1991**, 1019. (c) Chi, Y. *J. Chin. Chem. Soc.* **1992**, *39*, 591. (d) Roland, E.; Bernhardt, W.; Vahrenkamp, H. *Chem. Ber.* **1986**, *119*, 256. (e) Bernhardt, W.; Vahrenkamp, H. *Organometallics* **1986**, *5*, 2388.

(35) (a) Morrison, E. D.; Steinmetz, G. R.; Geoffroy, G. L.; Flutz, W. C.; Rheingold, A. L. *J. Am. Chem. Soc.* **1983**, *105*, 4104. (b) Morrison, E. D.; Steinmetz, G. R.; Geoffroy, G. L.; Flutz, W. C.; Rheingold, A. L. *J. Am. Chem. Soc.* **1984**, *106*, 4788.